Research Article

SOHAG JOURNAL OF SCIENCES

https://doi.org/10.21608/sjsci.2024.254285.1161

Antimicrobial Efficacy Mediated by Mycogenic and Characterized Selenium Nanoparticles

Nourhan H. Khalaf[1,*], Abdallah M. A. Hassane[1], Bahig A. El-Deeb[2] and Nageh F. Abo-Dahab[1]

[1] *Department of Botany and Microbiology, Faculty of Science, Al-Azhar University, Assiut, Egypt.*
[2] *Department of Botany and Microbiology, Faculty of Science, Sohag University, Sohag 82524, Egypt.*
[*] *Email: noor91199691@gmail.com*

Received: 9th December 2023, **Revised:** 26th January 2024, **Accepted:** 10th February 2024
Published online: 29th March 2024

Abstract: Natural source nanostructures have attracted a lot of attention due to their diverse biological activities and low toxicity to people, animals, and the environment. In this research, *Penicillium chrysogenum* AUMC 14831 isolated from *Pancratium maritimum* was used to reduce sodium selenite (Na_2SeO_3) to selenium nanoparticles (Se^0), by reacting with fungal filtrate. Selenium nanoparticle characterization was performed using UV-visible spectroscopy and the color of fungal filtrate turned into ruby red when treated with sodium selenite and gave a peak at 300 nm based on its optical property and surface plasmon resonance. Nanoparticles' crystallinity was determined by X-ray diffraction (XRD) and indicated that the peaks were sharp and located at 2θ values 23.5°, 29.7°, 41.32°, 43.65°, 45.36°, 51.7°, and 65.22°. Transmission electron microscopy (TEM) demonstrated the form and SeNPs' size which appeared spherical with diameters between 9 and 18 nm. Fourier Transform Infrared Spectroscopy (FTIR) revealed the capping agent's functional groups in charge of the stability and activity of SeNPs. Biosynthesized selenium nanoparticles showed significant antibacterial and anticandidal action. Mycologically synthesized SeNPs are promising compounds as antimicrobial agents.
Keywords: Selenium nanoparticles, mycosynthesis, *Penicillium chrysogenum*, characterization, antimicrobial activity.

1. Introduction

Nanoparticles are described as either naturally occurring materials or artificial materials that comprise particles either as aggregates or separated, between one and one hundred nm in diameter **[1]**. Numerous fields have employed nanotechnology in medicine **[2]**, agriculture **[3]**, electronics **[4]**, photonics, information storage, catalysis, Environmental remediation, administration of drugs, chemical sensing and imaging **[5]**. Consequently, because of their characteristics such as proportions of surface area to volume, size, shape, and chemical compositions **[6]**. Metallic nanoparticles are distinguished by optical and magnetic properties, surface plasmon resonance, quantum confinement, and high surface energies. As a result, they have been employed in numerous applications **[7]**.

There are three ways to create metallic nanoparticles: chemically, physically, and biologically **[1]**. Physical techniques have drawbacks like being expensive, requiring high energy, pressure and temperature, high cost, less productivity, less stability, and high waste. These methods are not suitable for preparing familiar shapes and sizes of nanoparticles. Chemical methods are perilous because metal nanoparticle surfaces have potentially harmful chemicals adhered to them. In medical applications, it has side effects **[8-10]**. Biological methods are eco-friendly, commercially viable, clean, and safe for the environment. Biological methods include using of plants, bacteria, cyanobacteria, algae, and fungus for nanoparticle synthesis **[11]**.

Fungi have frequently reduced the metal salts to produce metal nanoparticles because of traits like high biomass production, ease of handling and cultivation, and the ability to produce a lot of quantities of enzymes, metabolites, and extracellular proteins. These molecules are responsible for the synthesis nanoparticles and forming capping agents that give nanoparticles their stability and activity **[12-14]**. The extracellular synthesis of selenium nanoparticles can be carried out by various fungi such as *Fusarium semitectum* **[15]**, *Penicillium corylophilum* **[16]**, *F. equiseti*, *Aspergillus quadrilineatus*, *A. terreus*, and *A. ochraceus* **[17]**.

Selenium nanoparticles have garnered significant interest in the domains of biomedicine and food science because they are more biocompatible and less toxic than elemental Se and selenite **[18, 19]**. SeNPs have demonstrated a variety of biological and medicinal properties, including antimicrobial properties **[20]**, anticancer **[19, 21]**, antiprotozoal **[22]**, and scavenging free radicals **[23]**. SeNPs garnered significant interest from scientists working in the photo-conducting along with the previously mentioned activities **[24]**, and catalytic pollution degradation **[25]**. As a result, they come highly recommended and are acknowledged as excellent prospects for a range of industrial, medicinal, and agricultural uses. The current research aimed to mycosynthesise, characterize, and evaluate the antimicrobial activities of different concentrations of selenium nanoparticles on bacterial and fungal strains.

2. Materials and methods

2.1. Fungal isolate

Endophytic *Penicillium chrysogenum* AUMC 14831 was isolated from *Pancratium maritimum* **[26]** and used for mycosynthesis of selenium nanoparticles.

2.2. Molecular identification of the fungal isolate

The fungal isolate was grown on Czapek's agar (CZA) medium and incubated for five days at 28°C **[27]**. DNA was extracted at Assiut University's Molecular Biology Research Unit using the Patho-gene-spin DNA/RNA extraction kit (Intron Biotechnology Company, Korea). SolGent Company, Daejeon, South Korea, provided sequencing and polymerase chain reaction (PCR) techniques. The reaction mixture contained the universal primers ITS1 (forward) and ITS4 (reverse), which were used to amplify the ITS regions of the rRNA gene for the isolate. ITS1 (5'-TCCGTAGGTGAA CCTGCGG - 3') and ITS4 (5'-TCCTCCGCTTATTGATATGC -3') were the two primer compositions. The purified PCR product was sequenced using the same primers after adding ddNTPs to the reaction mixture **[28]**. The obtained sequences were analyzed using the Basic Local Alignment Search Tool (BLAST) on the National Centre for Biotechnology Information (NCBI) website. Phylogenetic tree construction and sequence analysis were performed with MegAlign (DNA Star) software version 5.05.

2.3. Preparation of mycelial-free culture filtrate

After being grown aerobically in Czapeks' broth, the fungal biomass was incubated for five days at 28 °C with 150 rpm/min of continual shaking. The resulting fungal biomass was then repeatedly washed with double-distilled water after being purified using Whatman no. 1 filter paper. Next, 200 millilitres of sterile double-distilled water were used to soak 10 g of fungal mycelia in a 500 millilitre Erlenmeyer flask and gently shaked for 48 hours at 28 °C. Then, the filtrate was employed the producing nanoparticles.

2.4. Selenium nanoparticle mycosynthesis

The mycelial-free filtrate was treated with individual additions of sodium selenite stock solutions made in deionized water, culminating in a 1.5 mmol/L final concentration. After that, the flask was kept in the dark for seven days at 28 °C. Centrifugation was used to gather the resulting nanoparticles, and ultrasonication was used to distribute a specific weight in sterile double-distilled water to be utilized as stock solutions.

2.5. Selenium nanoparticle characterization

2.5.1. UV-visible (UV-Vis) spectroscopy analysis

By visually seeing the color shift that denotes the reduction reaction, the synthesis of SeNPs was observed. SeNPs were identified using UV-Vis spectroscopy (Jasco V-530, Japan) to detect the presence of distinct surface plasmon resonance bands.

2.5.2. Transmission Electron Microscopy (TEM) measurements.

A transmission electron microscope (JEOL/JEM-2100, HRTEM, Tokyo, Japan) was used to examine the shapes of the synthesized SeNPs. After dispersing SeNPs on copper grids using drop casting, the TEM specimen under examination was created and let to air dry at room temperature. The SeNPs size was determined using ImageJ software.

2.5.3. Fourier transform infrared spectroscopy (FTIR)

The fungal filtrate and SeNPs have been dried, powdered, and prepared the FT-IR spectrum by forming a thin potassium bromide tablet containing dried NPs. The functional groups on the surface of SeNPs were examined using FTIR (6100, Perkin-Elmer, Germany) throughout the 400–4000 cm^{-1} wavelength range, with a resolution of 4 cm^{-1}.

2.5.4. X-ray diffraction (XRD) analysis

To confirm XRD analysis for elemental SeNPs, an X-ray diffractometer (Panalytical X'PERT PRO, UK) with Cu kα-radiation (λkα = 1. 1.540562 Å) run at 30 mA and 40 kV and scanning diffraction style in the 2∅ of 5–90º range was used with powdered SeNPs.

2.6. Antimicrobial activity

2.6.1. Tested microorganisms

Gram-positive (*Staphylococcus aureus* ATCC 6538) and Gram-negative (*Escherichia coli* ATCC 8739, *Pseudomonas aeruginosa* ATCC 9027, and *Salmonella typhi* AUH 71) bacteria were among the tested microorganisms used in this study, in addition to fungal isolates including *Candida albicans* ATCC 10231, *C. albicans* TU 59, *C. albicans* TU 67, *C. glabrata* TU 52, and *C. glabrata* TU 54 were taken from the culture collection available at Botany and Microbiology Department, Faculty of Science, Assiut Branch, Al-Azhar University. These common isolates and strains were usually used in our laboratories as standard pathogenic microbes for various biological activities **[29-31]**. For twenty-four hours, Mueller Hinton broth was used to cultivate the bacterial strains and isolates at 37 ºC, on the other hand, the fungal isolates underwent two days of incubation at 25 ºC while being cultured in Sabouraud dextrose broth.

2.6.2. Agar well diffusion method

The good diffusion method was utilized to conduct the antimicrobial assay according to Jahangirian et al. **[32]** instructions. The diameter of the well was 8 mm, filled with 50 µL of well-distributed, by sonication, SeNPs at different concentrations (5000, 4000, 3000, 2000, 1000, 900, 800, 700, 600, 500, and 400µg/ mL). A negative control consisting of sterilized double-distilled water was employed, and 1 mg/mL of clotrimazole and 1 mg/mL of chloramphenicol were employed as the corresponding positive controls for fungi and bacteria, respectively. For testing antibacterial activity, Muller-Hinton plates previously inoculated with the bacterial strains' 24-hour-old broth cultures were utilized. For antifungal activity, Sabouraud dextrose plates that were previously inoculated with a fungus spore suspension (10^5 spore/mL) were utilized. Positive bioactivity is described as the well's surrounding inhibition zone's diameter, expressed in millimeters.

3.3. Results

3.1. Sequence Data for Fungal Isolate

ITS sequences of the rDNA from the fungal sample isolated for this study (*Penicillium chrysogenum* AUMC14831, GenBank accession no. OR835639) were used to create a phylogenetic tree, which was subsequently matched to closely related sequences obtained from GenBank. The isolated strain showed

99.82% identity and 100% coverage with several strains of the same species including the type of strain *P. chrysogenum* CBS 306.48 with accession no NR_077 145. *A. ochraceus* is included in the tree as an outgroup strain **(Fig. 1)**.

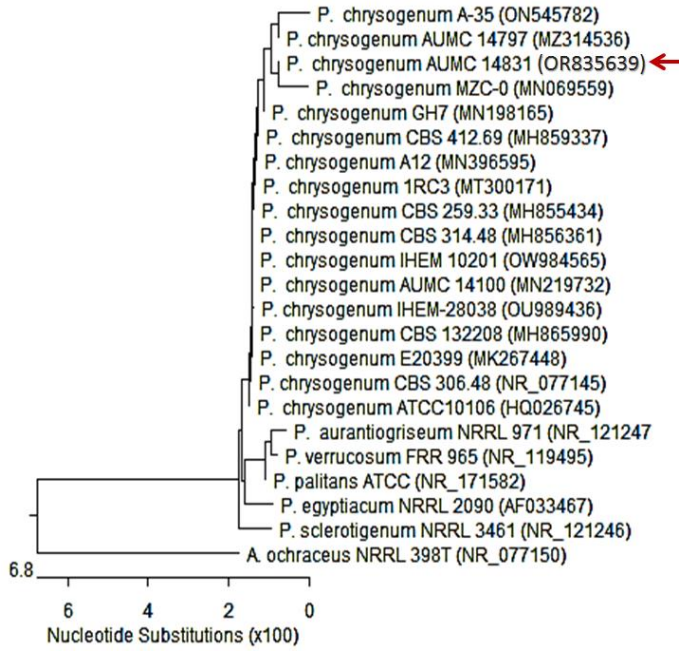

Fig. 1. *Penicillium chrysogenum* AUMC14831 phylogenetic tree based on the ITS sequences of the rDNA.

3.2. Characterization of biosynthesized selenium nanoparticles

3.2.1. UV-visible spectroscopy

After adding metal precursor (Na_2SeO_3) and incubating at 28 ºC for 7 days, the fungal biomass's color shift from colorless to ruby red was used to monitor the formation's success of Se-NPs **(Fig. 2A).** According to UV-visible wave analysis of SeNPs conducted over the 200–900 nm range, 300 nm was the location of the surface plasmon resonance band **(Fig. 2B).**

3.2.2. X-ray diffraction (XRD)

The XRD spectrum of selenium nanoparticles indicated that the peaks are sharp and are located at 2θ values 23.5°, 29.7°, 41.32°, 43.65°, 45.36°, 51.7°, and 65.22° were identified as 100, 101, 110, 122, 111, 201, 203, and 210 reflections **(Fig. 3)**. Sharp peaks showed good crystallite growth and the position of peaks indicate formation of pure Se nanoparticles.

3.2.3. Transmission electron microscopy (TEM)

The spherical shape and uniform distribution without significant agglomeration were confirmed by transmission electron micrographs **(Fig. 4)**. The examination of the SeNPs TEM micrograph data indicated that the particles' diameters varied from 9 to 18 nm.

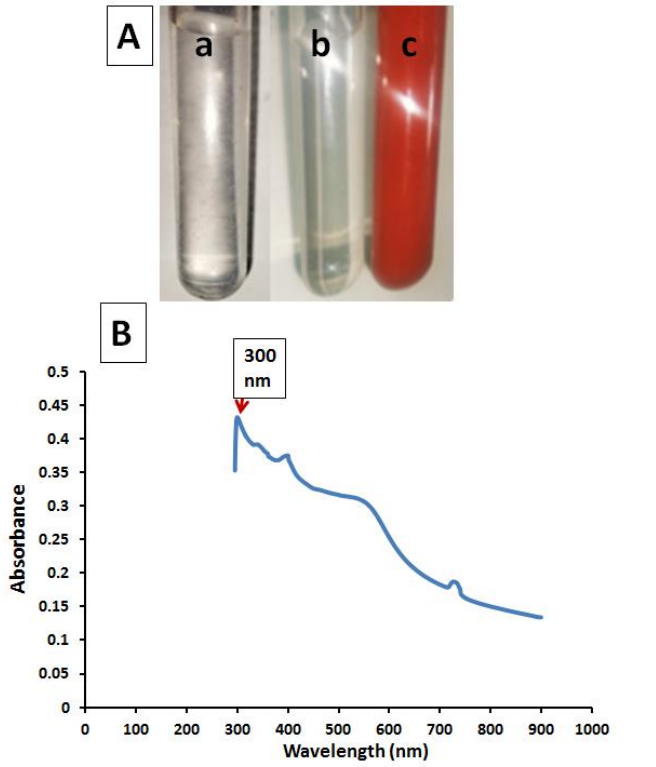

Fig.2. (A) Tubes containing a) sodium selenite, b) fungal filtrate without sodium selenite, and, c) fungal filtrate with sodium selenite. **(B)** UV–vis absorption spectrum of biosynthesized SeNPs.

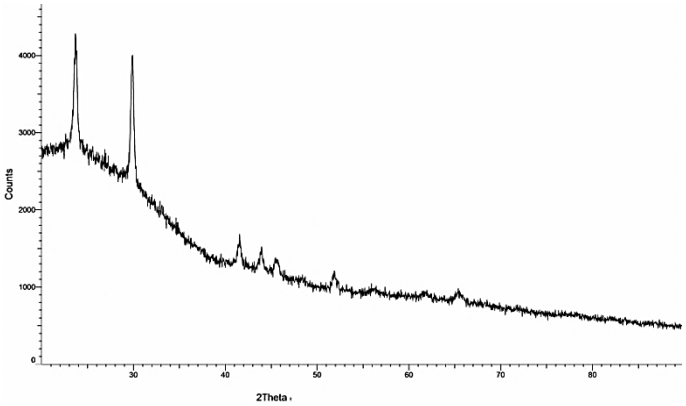

Fig. 3. XRD micrograph of biosynthesized SeNPs.

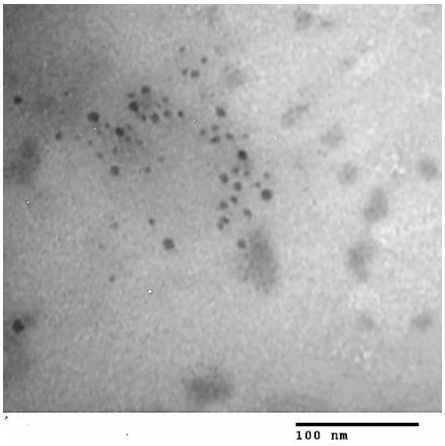

Fig.4. TEM images of SeNPs.

3.2.4. FTIR analysis of Ag NPs

The SeNPs' FTIR spectra revealed several bands, some of which were strong, the band centered at 2968.97 and 2921.48 cm^{-1} for aliphatic C–H stretching and the strong band at 1627.26 and 1533.33 cm^{-1} for carbonyl group C=O stretching were both visible in the spectrum. However, the C-O stretching group is attributed to the band with a center of 1231.99 cm^{-1}. While the sample's S=O stretching functional group is responsible for the strong band that is centered at 1024.98 cm^{-1} **(Fig. 5)**.

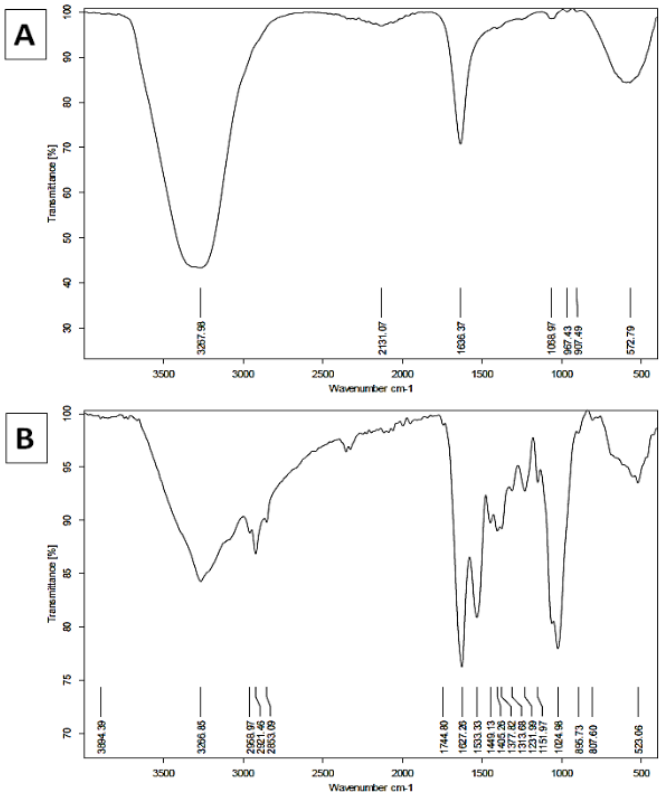

Fig.5. FTIR analysis **(A)** Fungal filtrate and **(B)** Biosynthesized SeNPs.

3.3. The biosynthesised silver nanoparticles' biological activity

Antibacterial activity of different concentration of SeNPs (5000, 4000, 3000, 2000, 1000, 900, 800, 700, 600, 500, 400) µg/mL inhibited the growth of the pathogenic bacteria *S. typhi* AUH 71, *E. coli* ATCC 8739, *P. aeruginosa* ATCC 9027, and *S. aureus* ATCC 6538, as shown in **Table (1)** and **Fig. (6)**. The inhibition zone's diameter ranged from (12.66 to 28.5 mm), (12 to 26.8 mm), (12.66 to 28.5 mm), and (12.83 to 28.5 mm), respectively. While antifungal activity of different concentrations of SeNPs (5000, 4000, 3000, 2000, 1000, 900, 800, 700, 600, 500, 400) µg/mL inhibited the growth of *C. albicans* ATCC 10231, *C. albicans* TU 59, *C. albicans* TU 67, *C. glabrata* TU 52, *C. glabrata* TU 54 with diameters of inhibition zones of (12 to 22.16 mm), (11.5 to 21.66 mm), (11.66 to 22 mm), (12.83 to 20.1 mm), and (15.66 to 20.5 mm), respectively **(Table 2)**.

4. Discussion

In this study, selenium nanoparticles were biosynthesized by *Penicillium chrysogenum* AUMC 14831 where this type of synthesis has an eco-friendly issue and are free from any organic solvents or hazardous substances during the biosynthesis process. Metabolites and extracellular proteins of fungal extracts are responsible for the synthesis nanoparticles and forming capping agent that gives nanoparticles their activity and stability **[12-14]**. After adding metal precursor (Na_2SeO_3) and incubating at 28±2 ºC for 7 days, the fungal biomass's color shift from colorless to ruby red was used to monitor the formation of SeNPs **[33]**. Biosynthezed selenium nanoparticles gave sharp peaks at 300 nm. Yang et al. **[34]** reported that mycosynthesized selenium nanoparticles displayed a peak at 245 nm, while Amin et al. **[35]** found that the one absorption peak measured at 262 nm for SeNPs made by *P. chrysogenum*. Salem et al. **[36]** detected SeNPs peak at 275 nm in wavelength. The spherical shape and uniform distribution with minimal agglomeration were confirmed by transmission electron micrographs.

The examination of the SeNPs TEM micrograph data revealed that the particles' diameters varied from 9 to 18 nm. According to Sakr et al. **[37]**, the size of the SeNPs biosynthesized by *Alternaria alternata* ranged from 30 to 150 nm. The biomass filtrate of the *P. chrysogenum* strain can produce spherical, homogeneous SeNPs measuring between 3 and 15 nm in size **[35]**. XRD analyses of the freshly formed SeNPs were carried out and the sharp peaks showed good crystalline and the position of peaks indicated formation of pure selenium nanoparticles. Based on X-ray diffraction peaks, they were crystalline **[24, 38, 39]**.

Table (1): Activities of selenium nanoparticles against Gram-positive and Gram-negative bacteria [after 24 hours]. Inhibition zone diameter in millimeters (mm).

Conc. (µg/mL)	Inhibition zone diameter (mm)			
	***S. aureus* ATCC 6538**	***E. coli* ATCC 8739**	***P. aeruginosa* ATCC 9027**	***S. typhi* AUH 71**
5000	28.50±0.50	26.80±1.75	28.50±0.50	28.50±1.50
4000	28.16±2.02	25.5±0.50	25.33±0.28	25.50±0.50
3000	27.66±2.51	25.33±0.58	23.50±0.50	25.16±0.76
2000	27.00±1.73	24.16±0.76	22.33±1.15	23.83±0.28
1000	25.33±0.58	24.00±0.86	19.00±1.00	23.16±.058
900	23.33±0.58	23.33±0.58	14.33±2.08	19.00±1.00
800	20.16±2.25	20.00±2.00	12.66±1.52	14.66±1.52
700	15.33±0.75	16.83±1.60	R	12.83±1.62
600	12.66±1.52	15.83±1.04	R	R
500	R	14.00±1.00	R	R
400	R	12.00±1.32	R	R
Control	38.00±1.73	18.60±0.76	14.80±0.76	27.10±1.04

Data were presented as the mean of three replicates (mean±SD); R: Resistant.

Table (2): Antifungal activities of the selenium nanoparticles against different *Candida* spp. [After 48 h]. Inhibition zone diameter (mm).

Conc. (µg/mL)	Inhibition zone diameter (mm)				
	C. albicans ATCC 10231	*C. glabrata* TU 54	*C. glabrata* TU 52	C. *albicans* TU 67	C. *albicans* TU 59
5000	22.16±0.76	20.50±0.86	20.10±0.28	22±2.0	21.66±1.52
4000	20.60±1.15	19.80±1.04	17.66±0.28	20.16±0.28	19.66±1.54
3000	20.66±1.15	17.66±0.28	15.50±0.86	19.66±1.15	19.50±1.32
2000	19.83±0.76	15.66±0.76	12.83±1.6	19.50±1.32	14.66±0.58
1000	15.66±1.15	R	R	15.16±0.28	11.5±0.50
900	12.66±2.08	R	R	11.66±0.57	R
800	12.00±1.32	R	R	R	R
700	R	R	R	R	R
600	R	R	R	R	R
500	R	R	R	R	R
Control	25±1.00	21.1±0.76	20±1.00	23.8±1.04	19.8±0.76

Data were presented as the mean of three replicates (mean±SD); R: Resistant.

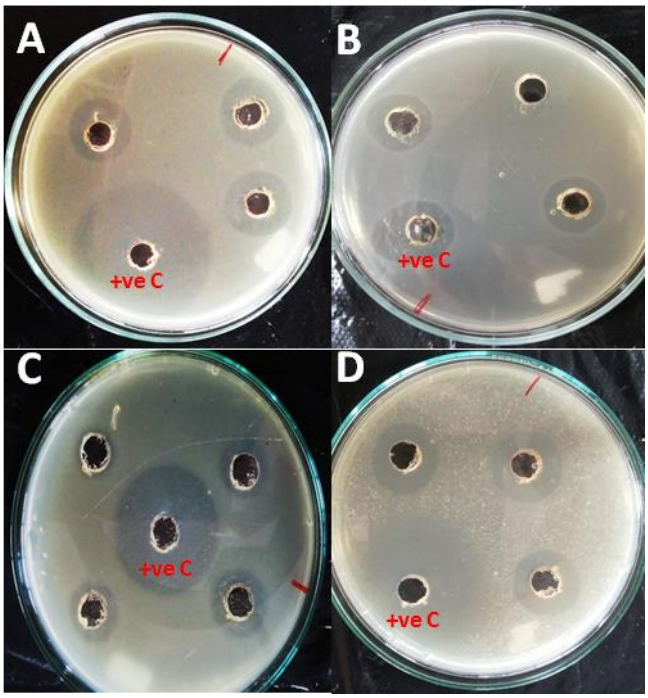

Fig. 6. Antimicrobial activity of biosynthesized SeNPs against **(A)** *S. aureus*, **(B)** *E. coli*, **(C)** *S. typhi*, and **(D)** *C. albicans*.

Regarding FTIR analysis, the proteins in the fungal extract might interact with the metal nanoparticles through their free amino or carboxyl groups **[40]**. It is important to understand though, that it is not just the size and shape of proteins, but the conformation of protein molecules that plays an important role **[40]**. The capping agent that forms on the nanoparticles from the fungal filtrate, which contains extracellular enzyme and biomolecules of proteins and metabolites, gives the biosynthesized solution of nanoparticles their characteristic stability **[41]**.

The current research indicates the biosynthesized nanoparticles' antimicrobial activity. Since the total surface area of nanoparticles is related to their antibacterial sensitivity, quicker penetration of microbial cells will occur as particle size decreases **[42]**. In this study, the activity of biosynthesized SeNPs was evaluated against bacterial strains of *S. aureus*, *S. typhi*, *P. aeruginosa*, and *E. coli* and fungal isolates such as *C. albicans*, and *C. glabrata*. Hussein et al. **[17]** reported that the minimum inhibitory concentration (MIC) of *A. quadrilineatus and A. ochraceus-synthesized* SeNPs against *C. albicans*, the most susceptible fungal pathogen to all SeNPs, was 62.5µg mL^{-1}. In the meantime, it has been discovered that several NPs interact with membranes or cell walls to let proteins, minerals, and genetic material escape the cell **[20, 43, 44]**. Moreover, NPs can stop the growth of microorganisms by producing reactive O_2 species **[23, 44, 45]**.

5. Conclusion

Within this research selenium nanoparticles are Biosynthesized by interacting between fungal filtrate of *Penicillium chrysogenum* and sodium selenite, resulting in stable and active selenium nanoparticles. These particles appeared spherical with a diameter varying between 9 and 18 nm. Herein, SeNPs exhibited significant antimicrobial action against various *Candida* spp. and bacteria strains which can be used as effective management to reduce pathogens development in medical applications.

CRediT authorship contribution statement: Conceptualization, N.A. and A.H.; methodology, N.K.; software, A.H.; validation, N.A. and B.E.; formal analysis, N.K.; investigation, B.E.; resources, N.K. and A.H.; data curation, A.H.; writing—original draft preparation, N.K. and A.H.; writing—review and editing, N.A. and B.E.; visualization, A.H.; supervision, N.A. and B.E. All authors have read and agreed to the published version of the manuscript.

Data availability statement: The data used to support the findings of this study are available from the corresponding author upon request.

Declaration of competing interest: The authors declare that they have no known competing financial interests or personal relationships that could have appeared to influence the work reported in this paper.

References

[1] J. Pulit-Prociak, M. Banach, *Open Chemistry*, 14 (2016) 76-91.
[2] H. Nosrati, R. A. Khouy, A. Nosrati, M. Khodaei, M. Banitalebi-Dehkordi, K. Ashraf-Dehkordi, S. Sanami, Z. Alizadeh, *Journal of Nanobiotechnology*, 19 (2021) 1–21.
[3] S. T. Thul, B. K. Sarangi, R. A. Pandey, *Expert Opinion on Environmental Biology*, 2 (2013) 2-7.
[4] E. Boisselier, D. Astruc, *Chemical Society Reviews*, 38 (2009) 1759-1782.
[5] S. Prabhu, E. K. Poulose, *International Nano Letters*, 2 (2012) 1-10.
[6] C. B. Murray, D. J. Norris, M. G. Bawendi, *Journal* of the American *Chemical Society*, 115 (1993) 8706-8715.
[7] E. C. Dreaden, A. M. Alkilany, X. Huang, C. J. Murphy, M. A. El-Sayed, *Chemical Society Reviews*, 41 (2012) 2740–2779.

[8] S. Mukherjee, B. Vinothkumar, S. Prashanthi, P. R. Bangal, B. Sreedhar, C. R. Patra, *RSC Advances*, 3 (2013) 2318–2329.
[9] S. Patra, S. Mukherjee, A. K. Barui, A. Ganguly, B. Sreedhar, C. R. Patra, *Materials Science and Engineering: C*, 53 (2015) 298–309.
[10] M. Ovais, N. Zia, I. Ahmad , A. T. Khalil, A. Raza, M. Ayaz, A. Sadiq, F. Ullah, Z. K. Shinwari, *Frontiers in Aging Neuroscience*, 10 (2018) 284.
[11] D. Singh, V. Rathod, S. Ninganagouda, J. Herimath, P. Kulkarni, *Journal of Pharmacy Research*, 7 (2013) 448–453.
[12] S. Chowdhury, A. Basu, S. Kundu, *Nanoscale Research Letters*, 9 (2014) 365.
[13] P. Azmath, S. Baker, D. Rakshith, S. Satish, S *Saudi Pharmaceutical Journal*, 24 (2016) 140-146.
[14] X. Zhao, L. Zhou, M. S. R. Rajoka, L. Yan, C. Jiang, D. Shao, J. Zhu, J. Shi, Q. Huang, H. Yang, M. Jin, *Critical Reviews in Biotechnology*, 38 (2018) 817–835
[15] A. Rahman, J. Lin, F. E. Jaramillo, D. A. Bazylinski, C. Jeffryes, S. A. Dahoumane, *Molecules*, 25 (2020) 3246.
[16] S. V. Kumar, A. P. Bafana, P. Pawar, A. Rahman, S. A. Dahoumane, C. S. Jeffryes, *Scientific Reports*, 8 (2018) 5106.
[17] H. G. Hussein, E. S. R. El-Sayed, N. A. Younis, A. A. Hamdy, S. M. Easa, *AMB Express*, 12 (2022) 68.
[18] P. A. Tran, N. O'Brien-Simpson, E. C. Reynolds, N. Pantarat, D. P. Biswas, A. J. O'Connor, *Nanotechnology*, 27 (2015) 45101.
[19] S. A. Wadhwani, U. U. Shedbalkar, R. Singh, B. A. Chopade, *Applied Microbiology and Biotechnology*, 100 (2016) 2555-2566.
[20] E-S. R. El-Sayed, H. K. Abdelhakim, A. S. Ahmed, *Bioprocess and Biosystems Engineering*, 43 (2020a) 797-809.
[21] Y. Huang, L. He, W. Liu, C. Fan, W. Zheng, Y. Wong, T. Chen, *Biomaterials*, 34 (2013) 7106–7116.
[22] S. Shirsat, A. Kadam, M. Naushad, R. S. Mane, *Rsc Advances*, 5 (2015) 92799–92811.
[23] E-S. R. El-Sayed, H. K. Abdelhakim, Z. Zakaria, *Materials Science and Engineering: C*, 107 (2020b) 110318.
[24] N. Srivastava, M. Mukhopadhyay, *Powder Technology*, 244 (2013) 26-29.
[25] J. Zhang, J. Spallholz, Toxicity of selenium compounds and nanoselenium particles. In General, Applied and Systems Toxicology. 2nd Ed. Wiley & Sons, New Jersy, USA, (2011).
[26] A. M. A. Hassane, S. M. Hussien, M. E. Abouelela, T. M. Taha, M. F. Awad, H. Mohamed, M. M. Hassan, M. H. A. Hassan, N. F. Abo-Dahab, A. A. El-Shanawany, *Frontiers in Bioengineering and Biotechnology*, 10 (2022) 930161.
[27] J. I. Pitt, A. D. Hocking, Fungi and Food Spoilage. 1st Ed. Springer, New York, USA, (2009).
[28] T. J. White, T. Bruns, S. Lee, J. Taylor, Amplification and Direct Sequencing of Fungal Ribosomal RNA Genes for Phylogenetics. In PCR Protocols: A guide to Methods and Applications. 1st Ed, Academic Press: San Diego, USA, (1990).
[29] H. Mohamed, A. Hassane, M. Rawway, M. El-Sayed, A. Gomaa, U. Abdul-Raouf, A. M. Shah, H. Abdelmotaal, Y. Song, *Archives of Microbiology*, 203 (2021) 4961–4972.
[30] A. A. Al Mousa, H. Mohamed, A. M. A. Hassane, N. F. Abo-Dahab, *Journal of King Saud University-Science*, 33 (2021) 101462.
[31] A. A. Al Mousa, M. E. Abouelela, N. S. Al Ghamidi, Y. Abo-Dahab, H. Mohamed, N. F. Abo-Dahab, A. M. A. Hassane, *Current Issues in Molecular Biology*, 46 (2023) 221–243.
[32] H. Jahangirian, M. Haron, M. H. S. Ismail, R. Rafiee-Moghaddam, L. Afsah-Hejri, Y. Abdollahi, M. Rezayi, N. Vafaei, *Digest Journal of Nanomaterials and Biostructures*, 8 (2013) 1263–1270.
[33] C. H. Ramamurthy, K. S. Sampath, P. Arunkumar, M. S. Kumar, V. Sujatha, K. Perkumar, C. Thirunavukkarasu, *Bioprocess and Biosystems Engineering*, 36 (2013) 1131–1139.
[34] L. B. Yang, Y. H. Shen, A. J. Xie, J. J. Liang, B. C. Zhang, *Materials Research Bulletin*, 43 (2008) 572–582.
[35] M. A. Amin, M. A. Ismail, A. A. Badawy, M. A. Awad, M. F. Hamza, M. F. Awad, A. Fouda, *Catalysts*, 11 (2021) 1551.
[36] S. S. Salem, M. M. G. Fouda, A. Fouda, M. A. Awad, E. M. Al-Olayan, A. A. Allam, T. I. Shaheen, *Journal* of *Cluster Science*, 32 (2021) 351–361.
[37] T. M. Sakr, M. Korany, K. V. Katti, *Journal of Drug Delivery Science and Technology*, 46 (2018) 223-233.
[38] A. R. Ingole, S. R. Thakare, N. T. Khati, A. V. Wankhade, D. K. Burghate, *Chalcogenide Letters*, 7 (2010) 485–489.
[39] G. A. Dorofeev, A. N. Streletskii, I. V. Povstugar, A. V. Protasov, E. P. Elsukov, *Colloid Journal*, 74 (2012) 675–685.
[40] A. Fouda, W. A. Al-Otaibi, T. Saber, S. M. AlMotwaa, K. S. Alshallash, M. Elhady, N. F. Badr, M. A. Abdel-Rahman, *Journal of Functional Biomaterials*, 13 (2022) 157.
[41] S. Mazumdar, R. Akter, D. Talukder, *Asian Pacific Journal of Tropical Biomedicine*, 5 (2015) 10-14.
[42] F. Martinez-Gutierrez, P. L. Olive, A. Banuelos, E. Orrantia, N. Nino, E. M. Sanchez, F. Ruiz, H. Bach, Y. Av-Gay, *Nanomedicine: Nanotechnology, Biology and Medicine*, 6 (2010) 681–688.
[43] R. Komal, B. Uzair, S. Sajjad, S. Butt, A. Kanwal, I. Ahmed, N. Riaz, S. A. K. Leghari, S. Abbas, *Materials Research Express*, 7 (2020) 55004.
[44] S. A. Mousa, E-S. R. El-Sayed, S. S. Mohamed, M. A. Abo El-Seoud, A. A. Elmehlawy, D. A. M. Abdou, *Applied Microbiology and Biotechnology*, 105 (2021) 741–753.
[45] R. K. Dutta, B. P. Nenavathu, M. K. Gangishetty, A. V. R. Reddy, *Colloids Surfaces B Biointerfaces*, 94 (2012) 143-150.